Metal-metal contact resistance measurements

Poyen Shen and Daniel Gall
Department of Materials Science and Engineering
Rensselaer Polytechnic Institute
Troy NY, 12180, USA

email: shenp4@rpi.edu, galld@rpi.edu

Abstract—The contact resistance at metal-metal (W, Mo, Ru, Co, TiN) interfaces is determined using a new method based on blanket superlattice thin films where the resistivity ρ parallel to the interfaces is measured as a function of superlattice period Λ to quantify the electron interface scattering. W(001)/Mo(001) superlattices show a continuous resistivity increase from 7.10 to 8.62 $\mu\Omega$ -cm with decreasing Λ = 50-1.7 nm, indicating a contact resistance of 2.6×10⁻¹⁶ Ω-m². Ru/Co multilayers show a much more pronounced increase from 15.0 to 47.5 μΩ-cm with Λ = 60-2 nm which is attributed to atomic intermixing leading to an interfacial Ru-Co alloy with a high measured $\rho = 61 \, \mu\Omega$ -cm and a Ru-Co contact resistance for interfaces deposited at 400 °C of 9.1 ×10⁻¹⁵ Ω-m². Ru/TiN and Co/TiN interface resistances are dominated by the high ρ for TiN, and are therefore proportional to the TiN thickness.

Keywords—contact resistance, multilayer, interconnects

I. INTRODUCTION

The interconnect resistance-capacitance (RC) signal delay in integrated circuits increases with each technology node [1]–[3] due to increasing electron scattering at surfaces [4]–[9], interfaces [10]–[12], and grain boundaries [13]–[16]. In addition, the contact resistance between different interconnect metals and/or metal-liner-metal interfaces is also expected to become an important contributor to the RC delay. However, metal-metal contact resistances are difficult to measure by conventional transitional-line-methods [17], [18] because the relatively low resistance would require sub-10-nm contact geometries. In this paper, we take an alternate approach to measure the contact resistance, using macroscopic four-point-probe measurements on blanket multilayer films. This quantifies the electron-interface scattering and yields, using appropriate models, the contact resistance.

We explore four different materials systems using multilayers: W/Mo, Ru/Co, Ru/TiN, and Co/TiN. The four elemental metals (W, Mo, Co, Ru) are already employed as conducting metals or are promising Cu-replacement candidates [19]–[22] and combining them to form vertical stacks or vertical-to-horizontal contacts may provide conductance and/or reliability benefits but requires more understanding of the interfaces including the contact resistance [7], [23]–[25]. TiN is a common liner [26]–[28] which, with conventional back-end-of-line (BEOL) processing, separates vertical and horizontal

The authors acknowledge funding from the Semiconductor Research Corporation (SRC) and DARPA under task Nos. 3085.001, 3137.19 and 3137.21, the National Science Foundation (NSF) and industry partners under grant No. 2328906, and from the NY State Empire State Development's Division of Science, Technology and Innovation (NYSTAR) through Focus Center-NY–RPI Contract C180117.

interconnects such that the metal-liner-metal contact resistance becomes an important quantity.

II. EXPERIMENTAL DETAILS

Metal and nitride layers are alternately deposited by DC sputtering in a three chamber ultra-high vacuum system [29], [30] to form 50-60 nm thick multilayers containing N = 2-60individual layers, corresponding to a bilayer period $\Lambda = 60-2$ nm. The substrates, MgO(001) and Al₂O₃(0001), are chosen in an attempt to achieve epitaxial growth, which reduces the grain boundary contributions to the overall resistivity [20], [31]–[33]. The deposition temperature $T_s = 900 \,^{\circ}\text{C}$ for W/Mo [34], $400 \,^{\circ}\text{C}$ for Ru/Co, 700 °C for Ru/TiN, and 400 °C for Co/TiN was chosen to optimize crystalline quality and minimize surface and interface roughness, as quantified by x-ray diffraction (XRD) and x-ray reflectivity (XRR) analyses. The sheet resistances were measured with a linear four-point-probe with 1.0 mm interprobe spacings and the overall multilayer resistivity was determined from the measured sheet resistance and thickness and appropriate geometric correction factors.

III. RESULTS

Fig. 1(a) is a plot of the measured resistivity ρ of metal multilayers vs the number of the interfaces. W(001)/Mo(001) multilayers are deposited on MgO(001) at 900 °C, resulting in epitaxial superlattices with sharp and smooth interfaces, as illustrated in Fig. 1(b) and determined from XRD and XRR measurements. Ru(0001)/Co(0001) multilayers are deposited on Al₂O₃(0001) at 400 °C, which results in 0001-textured superlattices with Ru-Co interfacial intermixing [see Fig. 1(c)] which is detected by an XRD alloy peak. The plotted resistivity exhibits an increase in ρ with increasing number of interfaces N. The lines through the datapoints are the result from curve fitting. More specifically, the red curve through the data points of W(001)/Mo(001) multilayers is based on an electron transport model which uses a interface transmission coefficient T to account for diffuse scattering at the W-Mo interfaces, and accounts for coherent transmission across multiple interfaces for electrons that do not scatter at phonons between traversing neighboring multilayer interfaces. The fitting procedure yields T = 0.8 ± 0.1 , which corresponds to a contact resistance at the W(001)-Mo(001) interface of $2.6 \times 10^{-16} \Omega$ -m². The fitting curve of the Ru(0001)/Co(0001) multilayers is based on an increasing amount of intermixed Ru-Co alloy with increasing number of interfaces. The completely intermixed alloy has a high resistivity $\rho = 61 \, \mu\Omega$ -cm, as measured from a co-deposited sample. The gradual composition changes at the interfaces cause no discrete interface electron scattering. Instead, the increasing Ru-Co intermixing with increasing number of interfaces results in the

plotted increasing resistivity. Data analysis yields a contact resistance for intermixed Ru-Co interfaces deposited at 400 °C of $9.1 \times 10^{-15} \Omega$ -m².

Figure 2 shows typical X-ray reflectivity result from Ru/TiN and Co/TiN multilayers. These two patterns are from multilayers containing five nominally 10-nm-thick Ru or four nominally 12.5-nm-thick Co layers which are separated by 1.0 nm thick TiN, resulting in total nominal thicknesses of 55 nm. The solid magenta line is the measured intensity vs scattering angle 2θ from the Ru/TiN multilayer, while the dashed line is the result from curve fitting with the Parratt formalism. The approximately 0.7°-wide fringes are due to the superlattice and provide a thickness of 11.4 nm for each bilayer consisting of one Ru layer and one TiN layer, yielding total measured thickness of 57 nm. The narrower fringes, particularly evident between $2\theta = 0.8^{\circ}$ -1.7°, are associated with the overall multilayer thickness of 57.4 nm, in excellent agreement with the 57 nm from the bilayer thickness. In contrast, the pattern from the Co/TiN multilayer (green) shows only weak and wide fringes, indicating a relatively high roughness > 1 nm of the Co/TiN interfaces. The high roughness may be associated with the formation of an interfacial CoTiN alloy which explains the measured (not shown) linear resistivity increase from 14.4-36.6 $\mu\Omega$ -cm with increasing N = 1-10. Conversely, the smooth interfaces in the Ru/TiN multilayers cause no additional resistivity.

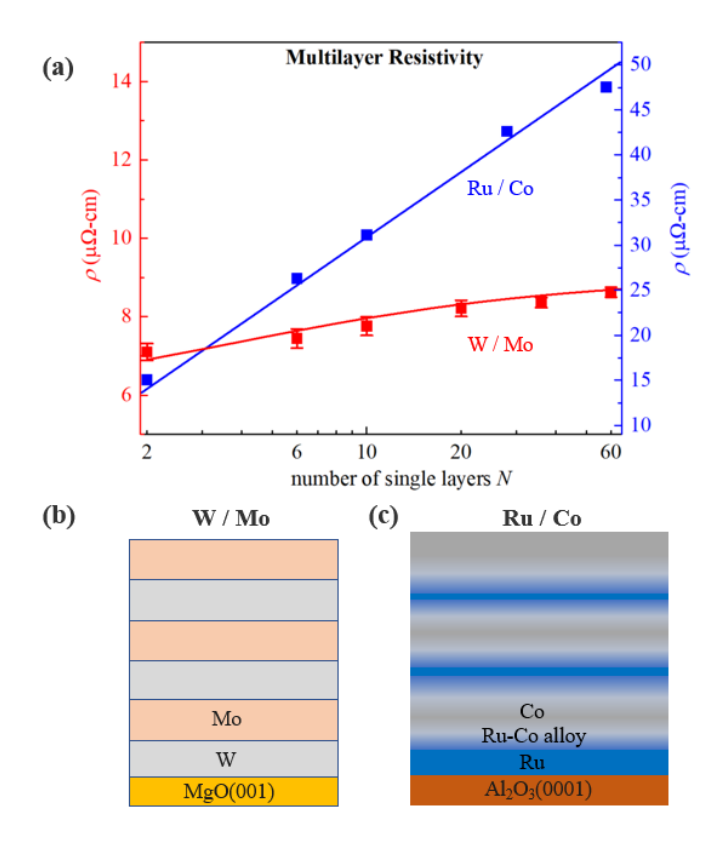


Fig 1. (a) Measured resistivity of 50-nm-thick W/Mo (red, left y-axis) and 60-nm-thick Ru/Co (blue, right y-axis) multilayers vs number of single layers N. Schematics of (b) W/Mo and (c) Ru/Co multilayers.

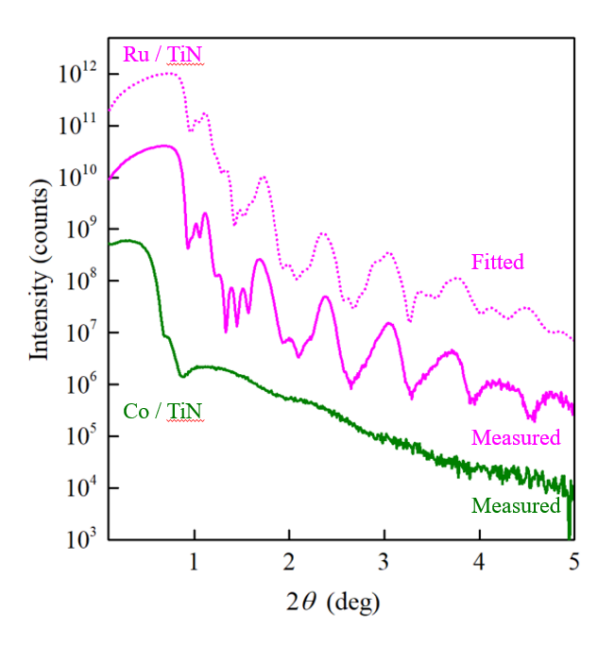


Fig 2. X-ray reflectivity curves from 50-nm-thick Ru/TiN and Co/TiN multilayer films. Solid lines indicate the measure intensity, and the dotted line is the result of curve fitting.

IV. CONCLUSIONS

The contact resistances of four materials systems are explored, using multilayer blanket films in combination with transport measurements parallel to the interfaces. The different materials systems exhibit different physical reasons dominating their contact resistance: W/Mo multilayers show sharp epitaxial interfaces such that the W-Mo contact resistance is determined by the match of the Fermi surfaces, resulting in a large 80% electron transmission coefficient and a correspondingly small $2.6\times10^{-16}~\Omega\text{-m}^2$ contact resistance. Ru/Co multilayers show the formation of Ru-Co interfacial alloys which dominate the contact resistance and lead to a relatively large $9.1\times10^{-15}~\Omega\text{-m}^2$. Ru/TiN and Co/TiN multilayers with 1.0 nm TiN layers indicate that the contact resistance of Ru-TiN-Ru and Co-TiN-Co interface stacks is dominated by the TiN resistivity and is therefore proportional to the TiN thickness.

REFERENCES

- [1] S. M. Rossnagel and T. S. Kuan, "Alteration of Cu conductivity in the size effect regime," *J. Vac. Sci. Technol. B*, vol. 22, no. 1, pp. 240–247, 2004, doi: 10.1116/1.1642639.
- [2] S. Dutta, K. Moors, M. Vandemaele, and C. Adelmann, "Finite Size Effects in Highly Scaled Ruthenium Interconnects," *IEEE Electron Device Lett.*, vol. 39, no. 2, pp. 268–271, 2018, doi: 10.1109/LED.2017.2788889.
- [3] A. Naeemi, C. Pan, A. Ceyhan, R. M. Iraei, V. Kumar, and S. Rakheja, "BEOL scaling limits and next generation technology prospects," in *Proceedings - Design Automation Conference*, 2014, pp. 1–6, doi: 10.1145/2593069.2596672.
- [4] J. S. Chawla, F. Gstrein, K. P. O. Brien, J. S. Clarke, and D. Gall, "Electron scattering at surfaces and grain boundaries in Cu thin films and wires," *Phys. Rev. B*, vol. 84, pp. 235423–1, 2011, doi: 10.1103/PhysRevB.84.235423.

- [5] J. S. Chawla and D. Gall, "Specular electron scattering at single-crystal Cu(001) surfaces," *Appl. Phys. Lett.*, vol. 94, no. 25, p. 252101, 2009, doi: 10.1063/1.3157271.
- [6] P. Y. Zheng, R. P. Deng, and D. Gall, "Ni doping on Cu surfaces: Reduced copper resistivity Ni doping on Cu surfaces: Reduced copper resistivity," *Appl. Phys. Lett.*, vol. 105, p. 131603, 2014.
- [7] P. Zheng, T. Zhou, and D. Gall, "Electron channeling in TiO2 coated Cu layers," *Semicond. Sci. Technol*, vol. 31, p. 055005, 2016, doi: 10.1088/0268-1242/31/5/055005.
- [8] E. Milosevic and D. Gall, "Copper interconnects: Surface state engineering to facilitate specular electron scattering," *IEEE Trans. Electron Devices*, vol. 66, no. 6, p. 2692, 2019, doi: 10.1109/TED.2019.2910500.
- [9] T. Zhou, P. Zheng, S. C. Pandey, R. Sundararaman, and D. Gall, "The electrical resistivity of rough thin films: A model based on electron reflection at discrete step edges," *J. Appl. Phys.*, vol. 123, no. 15, p. 155107, 2018, doi: 10.1063/1.5020577.
- [10] Y. Ke, F. Zahid, V. Timoshevskii, K. Xia, D. Gall, and H. Guo, "Resistivity of thin Cu films with surface roughness," *Phys. Rev. B - Condens. Matter Mater. Phys.*, vol. 79, pp. 155406–1, 2009, doi: 10.1103/PhysRevB.79.155406.
- [11] J. M. Purswani and D. Gall, "Electron scattering at single crystal Cu surfaces," *Thin Solid Films*, vol. 516, no. 2–4, pp. 465–469, 2007, doi: 10.1016/j.tsf.2007.07.146.
- [12] E. Milosevic, S. Kerdsongpanya, M. E. Mcgahay, B. Wang, and D. Gall, "The Resistivity Size Effect in Epitaxial Nb(001) and Nb(011) Layers," *IEEE Trans. Electron Devices*, vol. 66, no. 8, pp. 3473–3478, 2019, doi: 10.1109/TED.2019.2924312.
- [13] M. César, D. Liu, D. Gall, and H. Guo, "Calculated Resistances of Single Grain Boundaries in Copper," *Phys. Rev. Appl.*, vol. 2, p. 044007, 2014, doi: 10.1103/PhysRevApplied.2.044007.
- [14] M. César, D. Gall, and H. Guo, "Reducing Grain-Boundary Resistivity of Copper Nanowires by Doping," *Phys. Rev. Appl.*, vol. 5, p. 054018, 2016, doi: 10.1103/PhysRevApplied.5.054018.
- [15] A. Jog and D. Gall, "Electron Scattering at Surfaces and Grain Boundaries in Rh Layers," *IEEE Trans. Electron Devices*, vol. 69, no. 7, p. 3854, 2022, doi: 10.1109/TED.2022.3177153.
- [16] T. Zhou, A. Jog, and D. Gall, "First-principles prediction of electron grain boundary scattering in fcc metals," *Appl. Phys. Lett.*, vol. 120, no. 24, p. 241603, 2022, doi: 10.1063/5.0098822.
- [17] M. D. Pashley and J. B. Pethica, "Resistance measurement in metal-metal contact experiments Resistance measurement in metal-metal contact exp e r i men ts," *J. Phys. E Sci. Instrum.*, vol. 14, p. 584, 1981, doi: 10.1088/0022-3735/14/5/013.
- [18] H. H. Berger, "Contact Resistance and Contact Resistivity Contact Resistance and Contact Resistivity," *J. Electrochem. Soc. Conta*, vol. 119, p. 507, 1972, doi: 10.1149/1.2404240.
- [19] P. Y. Zheng, T. Zhou, B. J. Engler, J. S. Chawla, R. Hull, and D. Gall, "Surface roughness dependence of the electrical resistivity of W(001) layers," *J. Appl. Phys.*, vol. 122, no. 9, pp. 1–10, 2017, doi: 10.1063/1.4994001.
- [20] A. Jog, P. Zheng, T. Zhou, and D. Gall, "Anisotropic Resistivity Size Effect in Epitaxial Mo(001) and Mo(011) Layers," *Nanomaterials*, vol.

- 13, p. 957, 2023, doi: 10.3390/nano13060957.
- [21] E. Milosevic, S. Kerdsongpanya, M. E. McGahay, A. Zangiabadi, K. Barmak, and D. Gall, "Resistivity scaling and electron surface scattering in epitaxial Co(0001) layers," *J. Appl. Phys.*, vol. 125, p. 245105, 2019, doi: 10.1063/1.5086458.
- [22] E. Milosevic, S. Kerdsongpanya, A. Zangiabadi, K. Barmak, K. R. Coffey, and D. Gall, "Resistivity Size Effect in Epitaxial Ru(0001) Layers," *J. Appl. Phys.*, vol. 124, no. 16, p. 165105, 2018, doi: 10.1063/1.5046430.
- [23] C. L. Nies, S. K. Natarajan, and M. Nolan, "Control of the Cu morphology on Ru-passivated and Ru-doped TaN surfaces-promoting growth of 2D conducting copper for CMOS interconnects," *Chem. Sci.*, vol. 13, no. 3, pp. 713–725, 2022, doi: 10.1039/d1sc04708f.
- [24] C. Cancellieri et al., "Interface and layer periodicity effects on the thermal conductivity of copper-based nanomultilayers with tungsten, tantalum, and tantalum nitride diffusion barriers," J. Appl. Phys., vol. 128, p. 195302, 2020, doi: 10.1063/5.0019907.
- [25] T. Zhan et al., "Effect of Thermal Boundary Resistance between the Interconnect Metal and Dielectric Interlayer on Temperature Increase of Interconnects in Deeply Scaled VLSI," ACS Appl. Mater. Interfaces, vol. 12, no. 19, pp. 22347–22356, 2020, doi: 10.1021/acsami.0c03010.
- [26] L. G. Wen et al., "Atomic Layer Deposition of Ruthenium with TiN Interface for Sub-10 nm Advanced Interconnects beyond Copper," ACS Appl. Mater. Interfaces, vol. 8, p. 26119, 2016, doi: 10.1021/acsami.6b07181.
- [27] K. V Sagi, H. P. Amanapu, S. R. Alety, and S. V Babu, "Potassium Permanganate-Based Slurry to Reduce the Galvanic Corrosion of the Cu / Ru / TiN Barrier Liner Stack during CMP in the BEOL Interconnects," ECS J. of Solid State Sci. Technol., vol. 5, p. 256, 2016, doi: 10.1149/2.0141605jss.
- [28] J. S. Chawla, X. Y. Zhang, and D. Gall, "Effective electron mean free path in TiN(001)," *J. Appl. Phys.*, vol. 113, no. 6, p. 063704, 2013, doi: 10.1063/1.4790136.
- [29] M. Zhang, S. Kumar, R. Sundararaman, and D. Gall, "Resistivity scaling in CuTi determined from transport measurements and first-principles simulations," *J. Appl. Phys.*, vol. 133, no. 4, p. 045102, 2023, doi: https://doi.org/10.1063/5.0135132.
- [30] P. Fang, C. P. Mulligan, R. Jia, J. Shi, S. V. Khare, and D. Gall, "Epitaxial TiCx(001) layers: phase formation and physical properties vs C-to-Ti ratio," *Acta Mater.*, vol. 226, p. 117643, 2022, doi: https://doi.org/10.1016/j.actamat.2022.117643.
- [31] P. Zheng, B. D. Ozsdolay, and D. Gall, "Epitaxial growth of tungsten layers on MgO(001)," *J. Vac. Sci. Technol. A Vacuum, Surfaces, Film.*, vol. 33, no. 6, p. 061505, Nov. 2015, doi: 10.1116/1.4928409.
- [32] S. S. Ezzat *et al.*, "Resistivity and surface scattering of (0001) single crystal ruthenium thin films," *J. Vac. Sci. Technol. A*, vol. 37, no. 3, p. 031516, 2019, doi: 10.1116/1.5093494.
- [33] E. Milosevic and D. Gall, "Electron scattering at Co(0001) surfaces: Effects of Ti and TiN capping layers," *AIP Adv.*, vol. 10, p. 055213, 2020, doi: 10.1063/1.5145327.
- [34] P. Shen and D. Gall, "Electron scattering at interfaces in epitaxial W(001)-Mo(001) multilayers," under Review, 2024.